Journal of Computational Applied Mechanics 2024, 55(4): 683-697

DOI: 10.22059/jcamech.2024.376712.1104

RESEARCH PAPER

Modal Analysis of An Additively Manufacturing Scaled Wind Turbine Blade

Ahmed Kadhim Zarzoor [a, b], Ahmed Adnan Shandookh [a], Alaa Abdulhady Jaber [*, a], Bharat Bhushan [c]

[a] *Mechanical Engineering Department, University of Technology- Iraq, Baghdad, Iraq*
[b] *Mechanical Engineering Department, University of Al-Qadisiyah, Al-Qadisiyah, Iraq*
[c] *School of Engineering and Technology, Sharda University, Greater Noida, 201310, India*

Abstract

The efficiency and reliability work best in renewable energy systems highly dependent on the wellness of the designing of wind turbine blade. Additive manufacturing, namely 3D printing, opens new possibilities for manufacturing scaled models with complex geometries and advanced materials. This paper brings a significant study on the modal and fatigue life analysis of a wind turbine blade using ANSYS software which is 3D printed with the scale of 1:3.75, and further validated in the experimental view. Fabricated out of 0-degree-oriented carbon-fiber-reinforced PLA, the blade is extensively studied for structural integrity and vibrational response. Geometric and dynamic scaling laws are applied to ensure an accurate representation of full-scale blade behavior in scaled models. Modal analysis in ANSYS Workbench elucidates mode shapes and frequencies, while fatigue life analysis assesses structural durability under realistic loading conditions. Experimental testing employs precision instrumentation, validates numerical predictions, and confirms enhancements in structural integrity achieved through design modifications. The findings underscore the efficacy of additive manufacturing and iterative design optimization in advancing wind energy infrastructure, exemplifying a symbiotic fusion of computational modelling and experimental validation.

Keywords: Additive Manufacturing; Fatigue Life; Modal Analysis; Scale Law; Structural Testing

1. Introduction

Renewable energy is obtained from naturally existing and replenishable sources that do not diminish when utilized. These energy sources are sustainable over the long term and have a significantly lower environmental impact compared to fossil fuels and other forms of energy that cannot be replenished naturally. Renewable energy technologies harness the power of nature to generate electricity, heat, or other forms of energy. These technologies are considered environmentally friendly due to their minimal greenhouse gas emissions and absence of air pollution during energy production. Additionally, they are not subject to the same resource depletion issues as fossil fuels, making them a sustainable and reliable power source for the future [1-7].

Among all the renewable energy sources, wind power is the most popular and rapidly expanding. High-power

[*] Corresponding Author, email: alaa.a.jaber@uotechnology.edu.iq

wind turbines are needed to solve the energy issue with wind turbine technology; as a result, their designs should incorporate bigger blades and taller towers to accumulate more energy throughout their lifespan. On the other hand, wind turbines become more flexible as their towers or blades lengthen[8]. Consequently, the entire construction of a wind turbine will be more susceptible to environmental pressures, particularly dynamic excitations from wind, currents, and ocean waves. The system's natural frequencies may be approached by the excitation frequency, which could cause resonance and raise the fatigue stress on the system's flexible components. Thus, natural frequencies and the accompanying mode forms of wind turbines, or their dynamic features, are crucial to the design and operation of these structures [2, 9-11].

The most important part of the wind turbine system is usually thought to be the rotor's blades [2-4]. As a result, when designing a structure, designers need to take the blades' fatigue life into account and test the completed structure. The Germanischer Lloyd (GL) regulations and the IEC 61400-1 international specification [12, 13] specify structural design requirements such as minimum blade tip clearance limit, strain limits along the fiber direction, surface stress limit, and fatigue lifetime over 20 years. Since wind turbines need to have a long operating life of 20 to 30 years to be economically viable, the fatigue requirement frequently influences the design of a wind turbine's main structural components. Cycles to failure, or the number of large loads that a structure can withstand before cracks start to show or grow to an acceptable length, is how fatigue life is typically described.

In experimental modal analysis, input and response signals are measured and analyzed to examine the structural and dynamic properties of a kinetic system. The experimental test system's size is limited for large-scale rotor blades, though. While experimental information is more direct, theoretical modal analysis can be applied more broadly and simply. Various theoretical approaches exist, including finite element analysis (FEA) and numerical integral methods. A high-order system typically finds it challenging to compute modal characteristics using an integral method. Structural dynamic analysis has made extensive use of Finite Element Analysis (FEA), an approach that is both more accurate and convenient [14, 15].

Wind turbine components have been developed into tiny models and full-scale prototypes by the wind power sector through the use of Additive Manufacturing (AM) and various rapid prototyping techniques [16-24]. With the use of repeated layer-by-layer deposition, additive manufacturing can fabricate objects with complex geometries that would be too difficult to create with conventional manufacturing techniques [25]. Utilizing AM technologies opens up a vast array of design spaces for exploration and makes it easier to construct features at multiple hierarchical scales with customized material processing at different zones [26].

The American Society for Testing and Materials (ASTM) [27] has described seven classes of additive manufacturing (AM) procedures, which include material extrusion, material jetting, sheet lamination, vat photopolymerization, powder mattress fusion, and direct energy deposition. Among these, fused deposition modelling (FDM), a kind of material extrusion technique, is the most common method for polymeric applications [9, 28, 29]. FDM, additionally referred to as fused filament fabrication (FFF), uses a continuous filament of a thermoplastic polymer that is heated to a semi-solid state and then extruded on a surface or over previously deposited layers[29, 30]. While components printed through FMD show off the confined decision, constrained surface finishing, and anisotropy, this method can be done in low-cost equipment, bearing in mind the manufacturing of absolutely practical components with a couple of customizable substances [31, 32].

As a significant renewable energy source, wind turbines are becoming more and more important, and getting the most out of their designs is essential to maximizing performance and efficiency. [33] use QBlade software to analyze the effects of shell thickness, spar thickness, and spar position on wind turbine blade mass and modal shape. Results show increasing shell thickness improves stiffness while increasing spar thickness enhances blade strength and stiffness. Altering spar position affects load distribution and blade modal shapes.

This paper provides an in-depth study on the dynamic response and fatigue lifetime of a reduced scale wind turbine blade through both numerical analysis and experimental testing. At 1:3.75 scale, the blade is one of the largest in the world to be constructed via additive manufacturing, using carbon fiber-reinforced polylactic acid (PLA) due to its good balance of mechanical properties and sustainability. In this work, ANSYS software has been used for performing numerical simulations which offers a cost-effective and efficient way to forecast the full-scale characteristics of variable parameters based on the scaled model studies. This method has the remarkable appeal of a medium between the difficulty associated with a full-scale experimental testing of a prototype and the lack of context for dynamical structural behavior.

Also, experimental investigations are carried out with high precision instrumentation to validate the numerical results and illustrate the blade behavior in detail. Through controlled impact, excitation, and rigorous data analysis techniques such as the Fast Fourier Transform, modal frequencies and structural responses are accurately captured and evaluated. By bridging the gap between numerical simulations and experimental testing, this paper aims to contribute to the advancement of wind turbine blade design and additive manufacturing techniques. The insights gained from this study hold significant implications for enhancing the efficiency, reliability, and sustainability of wind

energy systems.

The outline of paper is organized as a section 1 an introduction about the importance of renewable energy and need for optimized wind turbine blade design. Section 2 shows the geometry of wind turbine blade. section 3 illustrates the scaling laws for wind turbine blades. Section 4 the numerical modeling of wind turbine blade which includes the geometry, materials properties, and boundary condition. Section 5 the experimental testing to evaluate structural integrity. Section 6 results and discussion. Finally, the discussion section.

2. Wind turbine blade model

The wind turbine blade described in this research is a scaled model from the original blade length of 1.5 meters and a cross-section of SG6043 airfoil[34]. Table 1 shows the properties of the blade which show the values of twist angle and chord length at each section of blade. The blade is constructed from 0-degree-oriented carbon fiber-reinforced polylactic acid (PLA) and consists of three main parts: skin, spar, and rib, as shown in Fig 1. The skin is the outermost layer of the blade that interacts with the airflow, while the spar is a central structural component that provides the blade with bending stiffness and torsional rigidity. Ribs are secondary structural components that are placed along the length of the blade to provide additional stiffness and support.

Table 1 provided detailed information about the properties of wind turbine blade at each section profile which consists of SG6043 airfoil, twist angle varies between 16.218 to 0.22 degree and chord length from (244.42 to 62.92) mm.

Table 1: Wind turbine blade model.

Profile	SG6043	Diameter=3000mm
r/R	Twist [deg]	Chord [mm]
0.132	16.218	244.42
0.193	24.132	211.75
0.253	19.922	208.12
0.312	13.523	142.78
0.37	11.503	130.68
0.43	9.145	121
0.492	7.293	104.06
0.551	5.946	91.96
0.611	5.104	84.7
0.673	4.43	82.28
0.73	4.093	78.65
0.792	2.241	70.18
0.852	2.409	72.6
0.912	1.736	71.39
1	0.22	62.92

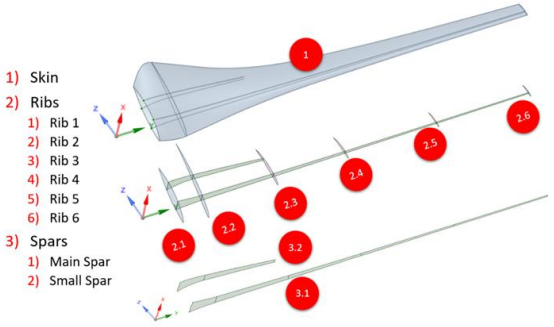

Fig 1: The internal structure of the blade.

3. Scaling laws for wind turbine blade

Scaled wind turbine blade models must adhere to scaling laws that ensure the physical and mechanical properties accurately represent those of full-scale blades. Scaling laws are essential in the design and testing of wind turbine blades to ensure that scaled-down models accurately represent the behavior of full-scale blades. These laws govern the relationships between the dimensions, forces, and performance of scaled models and their full-scale counterparts. Properly applied scaling laws help researchers and engineers obtain meaningful and reliable data from scaled testing. The wind turbine blade is scaled in this investigation using the same formulations found in the literature. A scale factor of Scale Factor Selection: We selected a geometric scale factor of λ was used to uniformly downscale the dimension of the turbine blade that is been investigated. Since, the material properties of the 3D printed material also differ from convention material due to printing induce defects. A correction has also been applied to the material properties to reflect the dynamics of full-scale mode. Nevertheless, the process of scaling is intricate and frequently accompanied by challenges. The objective of this research was to reduce the cost of manufacturing while maintaining the blade's geometric properties by scaling the blade. This was accomplished by modifying the Creality 3D printer that was available on site in the university research facility. The printer's test section was lengthened to accommodate the blade's extended length, enabling the blade to be produced in a single piece. Critical information, along with equations for geometric, dynamic, and structural scaling of wind turbine blades for experimental testing, is provided below [34-37].

3.1. Geometric scaling laws

Linear scaling is typically employed when scaling the dimensions of a wind turbine blade for experimental testing, such as its length (L), chord (c), and thickness (t). The length scale factor (λ) is used to represent the scaling relationship. Equations 1 to 3 represent the linear length scaling laws (1: λ) for wind turbine blade scaling.

$$L_{scaled} = \frac{L_{full-scale}}{\lambda} \tag{1}$$

$$c_{scaled} = \frac{c_{full-scale}}{\lambda} \tag{2}$$

$$t_{scaled} = \frac{t_{full-scale}}{\lambda} \tag{3}$$

The cross-sectional area (A) of the blade scales with the square of the length 14 scale factor (λ). Similarly, the volume of the blade scales with the cube of the 15-length scale factor (λ). Equations 4 and 5 represent area scaling $(1:\lambda^2)$ and volume 16 scaling $(1:\lambda^3)$ law for wind turbine blade scaling.

$$Area_{scaled} = \frac{Area_{full-scale}}{\lambda^2} \tag{4}$$

$$Volume_{scaled} = \frac{Volume_{full-scale}}{\lambda^3} \tag{5}$$

3.2. Dynamic scaling laws

Dynamic similarity ensures that the aerodynamic forces acting on the scaled model are equivalent to those on the full-scale blade. To achieve dynamic similarity, the scaling factors for velocity (V), density (ρ), and dynamic viscosity (μ) must be considered. These factors are typically derived from the Reynolds number (Re). The Reynolds number (Re) for a wind turbine blade is a dimensionless parameter that characterizes the flow of air around the blade. It helps determine whether the flow is laminar or turbulent and plays a crucial role in predicting aerodynamic performance. Equation 6 provides the relation for calculating the Reynolds number of full-scale wind turbine blades.

$$Re = \frac{\rho.V.L}{\mu} \tag{6}$$

Here, V is the velocity of air at which the wind turbine blade is operational, and L is the characteristic length and a measure of the length scale associated with the flow. For wind turbine blades, it is often defined as the length of the blade from the root to the tip or some other relevant length, and μ is the dynamic viscosity of air approximately equal to $1.789x10^{-5}\,\frac{kg}{m\cdot s}$ at 15°C. To maintain dynamic similarity, the Reynolds number must be kept constant between the scaled model and the full-scale blade, which means $Re_{scaled} = Re_{full-scale}$. If the density of air is kept constant, then the velocity of air at which the experimental testing of the scaled model should be conducted should be calculated

using Equation 7.

$$V_{scaled} = \frac{Re.\mu}{\mu.L_{scaled}} \tag{7}$$

In addition, the tip speed ratio must also be kept constant for full-scale and scaled models. To keep the tip speed ratio constant, Equations 8 to 11 can be used.

$$V_{tip,full-scaled} = R.\omega \tag{8}$$

$$V_{tip,\ scaled} = \frac{V_{tip,full-scaled}}{\lambda} \tag{9}$$

$$R_{scaled} = \frac{R}{\lambda} \tag{10}$$

$$\omega_{scaled} = \frac{V_{tip,scale}}{R_{scaled}} \tag{11}$$

Where R is the radius and ω is the angular velocity of the full-scale blade. λ is the length scale factor discussed in geometric scaling laws. By applying these scaling laws, scaled wind turbine blade models can be designed for experimental testing that faithfully represents the behaviors of full-scale blades. Properly scaled models ensure that the insights gained from testing apply to real-world wind turbine systems. The parameters discussed above are compared and shown in Table 2.

Table 2. parameters of full-scale and scaled blade

Scaling factor (λ)	3.75	
	Full scale	Scaled
Radius (m)	1.5	0.4
Reynolds number	308133	82168
Velocity air (m/sec)	3	3
Tip speed ratio	7	7
Omega (rad/sec)	14	52.5

4. Numerical Modelling of Wind Turbine Blade

The numerical analysis was performed on a 1:3.75 scale wind turbine blade to calculate the structural integrity of the scaled down blade in terms of modal frequencies, fatigue life, and safety factors. These parameters help in conducting successful experimental tests by providing information regarding the structural behavior of the blade before going into prototype development using additive manufacturing/3D printing. The numerical analysis for this purpose was conducted in ANSYS Workbench.

4.1. Geometry and Materials Properties

Carbon fibre-reinforced polylactic acid filament would be used as the material of the scaled blade prototype, therefore, the material characteristics were imported into ANSYS Workbench Engineering Database. The material was created with the properties mentioned in Table3. The 0-degree-oriented carbon fiber-reinforced PLA (CFR-PLA) was selected for the scaled-down blade because it has better mechanical properties than PLA. Additionally, additive manufacturing (AM) techniques were used for rapid prototyping, allowing for precise control over blade geometry and fiber orientation. The fibers are aligned along the load route in the 0-degree orientation, which maximizes the strength and stiffness of the material in that specific direction. It is worth heightening that, the turbine blade resembles the cantilever beam. One end is fixed while the other is allowed to deform. To ensure the structural integrity in the bending, the fiber must be placed in the axis parallel to the length of turbine blade. Given that the objective of this study was to demonstrate the application of additive manufacturing for rapid prototyping and experimentation, it is anticipated that a significant quantity of unused blades may accumulate in inventory over time. Therefore, CFR-PLA is well-suited for this application because of its environmentally favourable characteristics [5]. Polylactic acid (PLA) is a type of polymer that can naturally break down, making it an eco-friendlier choice than the petroleum-based resins commonly used in traditional composites. When combined with carbon fiber reinforcement (CFR), CFR-PLA becomes an even more environmentally beneficial option. This might be a crucial factor for smaller-scale models utilized in educational environments or scientific investigations. The original scale comparison of the full scale and scaled blade can be seen in Figure. The shapes and internal layout of 4 different structural designs of the blade where 'BASELINE' means the staring structural design and later it was optimized using 3 more structural designs shown in

Fig 3. ANSYS workbench has been utilized and simulations were performed on static structural module of the ANSYS. Due to complex geometry and peculiar mechanical behaviour of the 3D printed polymer non-linear analysis was conducted to incorporate the effect of geometric and material nonlinearity. 3D printed polymer composites manufacture the part layer by layer, thus making the structure highly orthotropic in nature. To incorporate this effect, a material model was developed in ANSYS material designer, and the properties were further imported ANSYS ACP to perform layering and then to the static structural module for the analysis.

Table 3. Carbon Fiber Reinforced PLA Material Properties

Density (Kg/m3)	1300
Orthographic Modulus (MPa)	
Modulus in X direction	4150
Modulus in Y direction	7556
Modulus in Z direction	4150
Poisson Ratio in X direction	0.16
Poisson Ratio in Y direction	0.388
Poisson Ratio in Z direction	0.16
Shear Modulus in X direction	1270
Shear Modulus in Y direction	1270
Shear Modulus in Z direction	1270
Tensile Yield Strength (MPa)	51
Tensile Ultimate Strength (MPa)	53

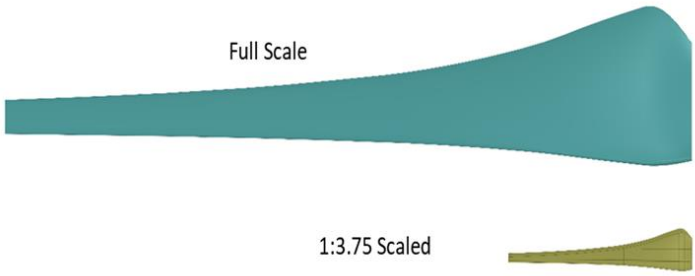

Fig 2: Comparison of full scale and scaled wind turbine blade

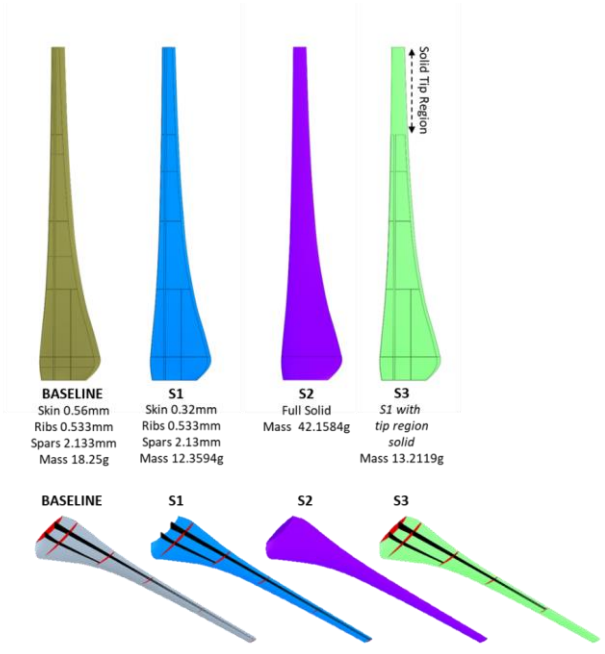

Fig 3: Comparison of Structural design of Scaled Blades

4.2. Modal Analysis

The modal analysis was performed in ANSYS Workbench using the Static Structural Modal Tool. Fixed support boundary condition was applied at the root part of the blade. Mesh was modeled as deformable structure with large deflections off and modal frequencies were searched for the range of 0-10000 Hz.

4.3. Fatigue Life Analysis

Wind turbine blades are subjected to complex loading conditions during their operational lifetime, experiencing a combination of aerodynamic forces, gravitational loads, and mechanical torques. The fatigue life analysis in this study considered realistic loading conditions that wind turbine blades experience during operation. Thus, for this purpose all the actual loads act on the turbine blade. The aerodynamic loads at optimum tip speed ratios with highest output power were considered and modelled in FEM analysis. These aerodynamic loads include the torque on the blade in addition to the axial and normal forces in the blade. Further, the figure below depicts the boundary condition of FEA in which the fixed constrain is applied to the root, further aerodynamic forces computed using numerical formulation was also applied at the centre of pressure of the blade. In addition to that, a torque generated due to the aerodynamic loading and moment has also been applied to replicate the actual working mechanism of the turbine blade. The numerical analysis employed fixed support at the root, a torque of 6 Nm at the root, a force of 10 N at the centre of the pressure point, and a rotation velocity of 501 RPM. The boundary conditions can be seen in Fig 5. Stress life computations were performed using the Goodman theory, considering Equivalent (von Mises) stresses. This comprehensive approach accounts for both static and cyclic loading conditions, providing a realistic assessment of the blade's structural performance. The primary objective was assessing fatigue life and safety factors using Goodman theory with Equivalent (von Mises) stresses.

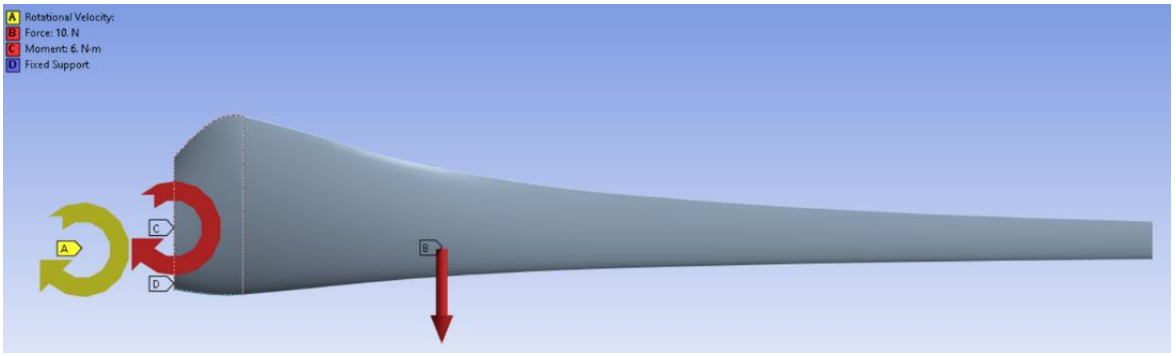

Fig 4: Boundary Conditions for Fatigue Life Analysis

The mesh was generated using hexagonal cells with fine resolution around corners and at thin or highly curved surfaces. The created model consists of 747693 elements, 1314620 nodes. The parameters for the mesh and the mesh are illustrated in Figure 5.

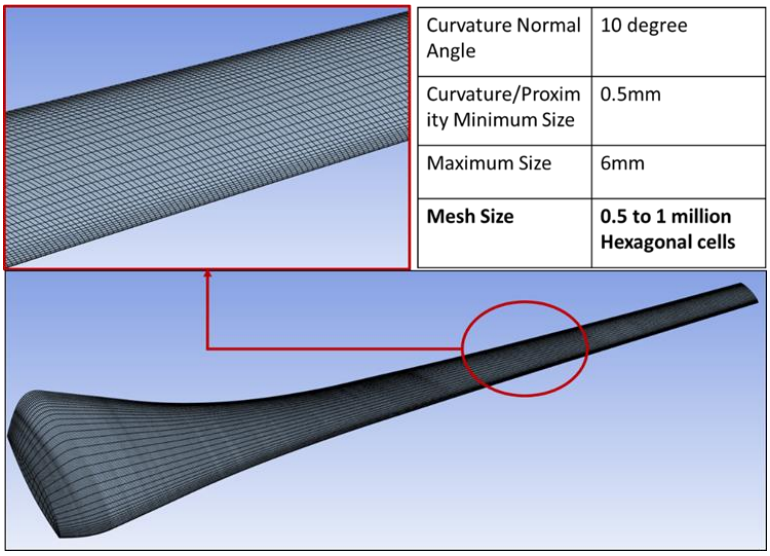

Curvature Normal Angle	10 degree
Curvature/Proximity Minimum Size	0.5mm
Maximum Size	6mm
Mesh Size	**0.5 to 1 million Hexagonal cells**

Fig 5: Boundary Conditions for Fatigue Life Analysis

5. Experimental Setup

In the pursuit of enhancing the capabilities of additive manufacturing for wind turbine blade production, Creality Ender-3 Pro 3D printer is used for manufacturing the wind turbine blades (baseline and optimize S1). In the subsequent phase of the study, the 3D-printed blades underwent rigorous experimental testing to ascertain their structural performance and dynamic characteristics, particularly focusing on the calculation of modal frequencies. The evaluation process employed a precision piezoelectric accelerometer in conjunction with an impact hammer sourced from ICP -(Instrumented Impact Hammers), a registered company renowned for its specialized instrumentation and measurement equipment Fig 6. High-quality experimental data were measured, and controlled strain experiments enabled time-distance trajectories for acceleration and displacement to be recorded in Fig.6. Time-series data from the strain hammer were used to show how the system responded to external stimuli in the form of time-dependent velocity and displacement profiles immediately following this, fast-Fourier transform (FFT) analyses was executed to transform the time-domain data to the frequency domain of the system, which would allow for the visualization of the modal frequencies from the printed structures as well as maps that are seen from this frequency spectrograph originated from the FFT-analysis This method would offer a comprehensive look at the vibrational modes and resonant frequencies of the system This method is capable of both identifying the modal frequencies and provided an enhanced tool to evaluate the system integrity and performance This while using a high-fidelity data acquisition by using a known accurate and reliable piezoelectric accelerometer and ICP impact hammer -Identified. The data collected was crucial to understanding. The subsequent sections will expound upon the intricacies of the experimental methodology, the nuances of data analysis, and the implications of the findings in the context of additive manufacturing for wind turbine blade production. The weight of the accelerometer should generally be no greater than 10 percent of the weight of the test structure. [38]. The mass of the printed scale wind turbine blade is 160 grams, while the mass of the accelerometer sensor is about 5 grams. This mass ratio is acceptable, as it does not affect the modal analysis results.

Sensitivity	±20%, 100 mV/lbf (22.5 mV/N)
Measurement Range	50 lbf pk (222 N pk)
Hammer Mass	0.17 oz (4.8 gm)

Fig 6: Apparatus used for experimental testing: [clockwise from top left] accelerometer, impact hammer, data acquisition card.

Table 4. Accelerometer sensor specification

Model number 352C03	ICP Accelerometer
Sensitivity (±10%)	1.02 mv/(m/s^2)
Measurement Range	± 4900m/s^2 pk
Frequency Range (±)	0.5 to 10,000 H_z
Frequency Range (±)	0.3 to 15,000 H_z
Resonant Frequency	≥ 50k H_z
Broadband Resolution (1 to 10000H_z)	0.005 m/s^2 rms
Non- Linearity	≤ 1%
Transverse Sensitivity	≤ 5%

Fig 7: Experimental testing (apparatus and model assembled)

6. Results and Discussion

6.1. Modal Analysis

The mode shapes of all designs shown in Fig 8 are predicted to be the same however with slight variations in shapes at low-frequency modes but observable variation in shape at mode 6. For this research only the first three modes are of utmost importance because these low frequency modes can cause resonance during real life application of wind turbines.

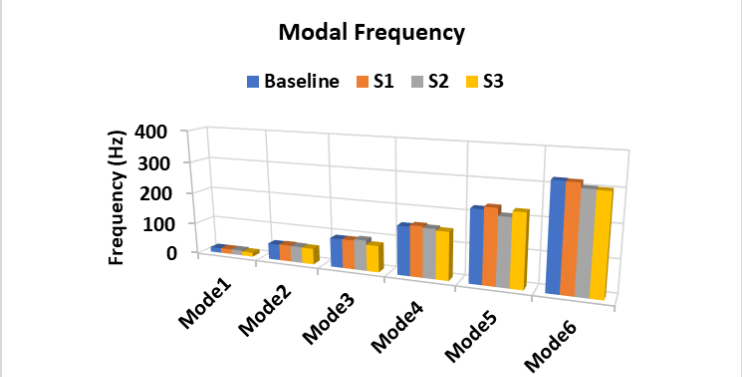

	Mode1	Mode2	Mode3	Mode4	Mode5	Mode6
Baseline	15.485	51.117	91.337	152.3	223.5	320.86
S1	15.771	52.36	91.556	157.21	231.28	319.47
S2	16.159	51.144	95.696	153.14	208.94	304.29
S3	13.446	49.97	82.701	148.83	225.66	302.46

Fig 8: Modal frequencies comparison of the blades

The comparison of modal frequencies is shown in Fig 8. It can be seen that the modal frequency of the first three modes is increased in S1 as compared to the baseline blade while reducing the weight of the blade as shown in Fig 3. The data of modal frequencies was then used to calculate the resonance factor of the blades using the rotation frequency of the blades which is 12 revolutions per second or 12Hz. The resonance factor of the 1st mode is of utmost importance because the 1st modal frequency is the lowest and can cause resonance in the blade. The structures are designed to keep the resonance factor below 0.95 so that resonance may not occur in blades. Fig 9 shows the comparison of the calculated resonance factors of the blades. It can be seen that the resonance factor is reduced in S1 and S2 blades in comparison to the Baseline blade. The increase of modal frequency and decrease in the resonance factor of S1 and S2 blade in comparison to the baseline blade shows that the structural dynamics of S1 and S2 blades are improved and optimized successfully. Resonance analysis for wind turbines typically involves calculating the natural frequencies and modes of vibration and then comparing these with the operating conditions to ensure that the turbine does not experience resonance-induced damage. Germanischer Lloyd Wind Energy GmbH's guidelines [37] likely incorporate methods for resonance analysis, which involve calculating the natural frequencies and modes of

vibration, and then ensuring that the turbine does not experience resonance-induced damage. to avoid the phenomenon of resonance, we have to check the condition given by the equation (12).

$$\frac{F_{rotation}}{F_{o,n}} \leq 0.95 \tag{12}$$

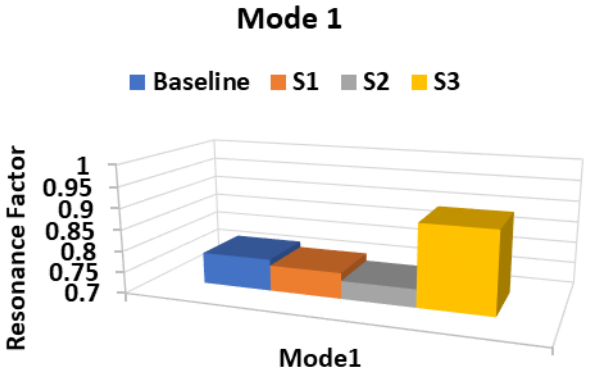

	Mode1
Baseline	0.774943494
S1	0.760890242
S2	0.742620212
S3	0.892458724

Fig 9. Resonance factor comparison of the blades.

The total deformation in the bending direction defines significantly the aerodynamic performance of the blade. For this purpose, the directional deformations were also calculated in modal analysis to see how the baseline blade and S1 blade compare. Fig 10 shows the directional deformation of the blades at multiple modes. It can be seen that by reducing weight, we have reduced the stiffness of the blade and hence the deformation of the S1 blade is higher in comparison to the Baseline blade at all modal frequencies.

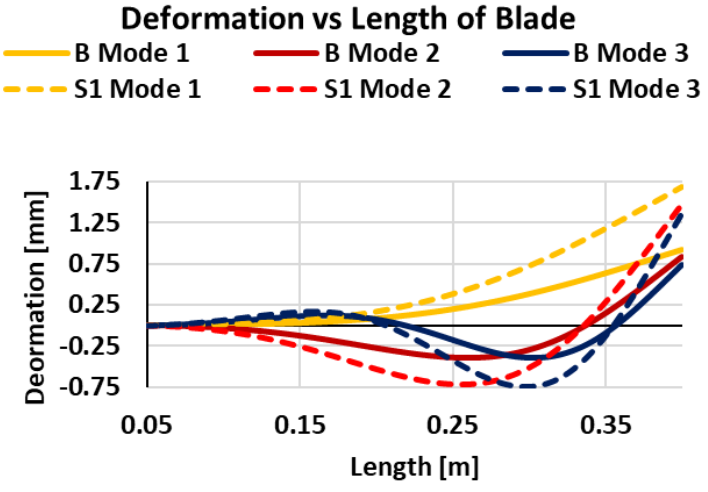

Fig 10. Directional Deformation in the bending direction of the blades at multiple modes.

6.2. Fatigue Analysis Results

The fatigue life and safety factor evaluations yielded noteworthy insights into the performance of the different blade designs. Figure 11 illustrates the fatigue life comparison among the blade configurations. S1 exhibits a superior fatigue life compared to the Baseline and S2 at 1.5 times the design load. However, at 100% of the design load S2 outperforms Baseline and S1. The values for the fatigue life of Baseline, S1 and S2 at 100% of the design load are compared in Table 4. This improvement can be attributed to the innovative design features incorporated into S1 and further enhanced in S2, highlighting the positive impact of design modifications on the blades' structural durability.

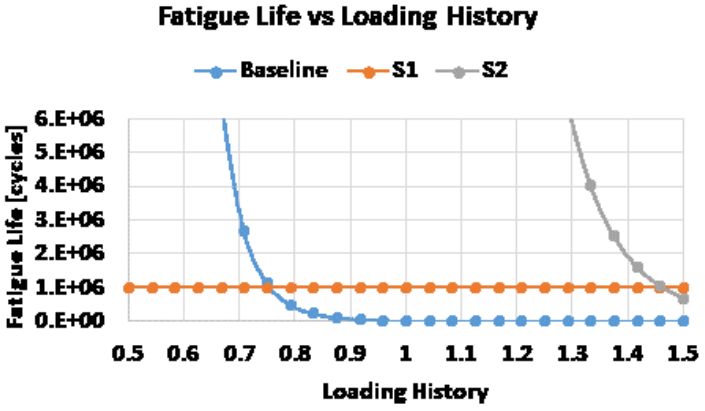

Fig 11. fatigue life of blade.

Examining Fig 12 which depicts the safety factors for the three blade configurations, a similar trend emerges. S1 demonstrates a higher safety factor than the Baseline, and S2 outperforms both, emphasizing the cumulative effect of design enhancements. The safety factor is a critical parameter in ensuring that the blade operates within its structural limits, preventing catastrophic failures. The observed improvements in safety factors underscore the success of the design modifications in enhancing the structural robustness of the wind turbine blades.

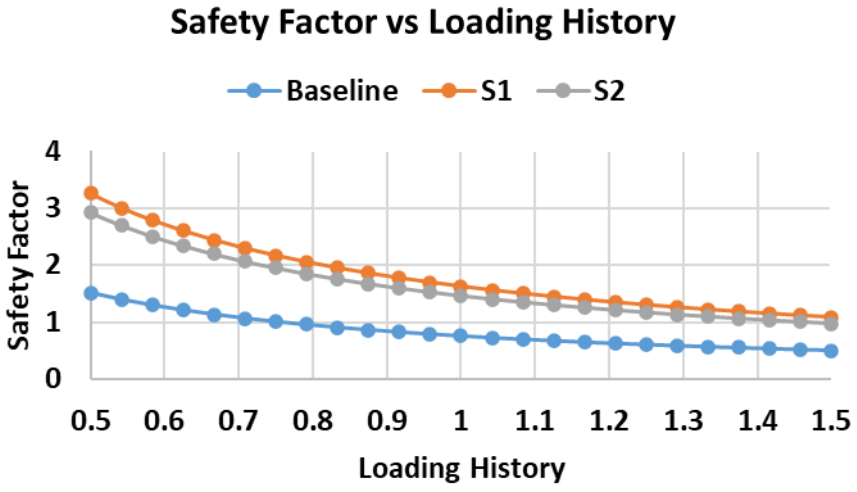

Fig 12. safety factors of the blades.

The fatigue life analysis and safety factor assessments substantiate the efficacy of design modifications in increasing the structural dynamics and fatigue life of the wind turbine blades. The iterative improvements from Baseline to S1 and further to S2 showcase the success of engineering interventions aimed at optimizing blade performance. These findings hold significant implications for the renewable energy sector, as increased fatigue life and safety factors contribute directly to the overall reliability and longevity of wind turbine systems. As we advance towards sustainable energy solutions, the continuous refinement of wind turbine blade designs proves to be a key

factor in maximizing efficiency and minimizing maintenance requirements.

Table 5. Fatigue testing results at design loading

Parameter at 100% Loading		
	Fatigue Life [cycles]	Safety Factor
Baseline	6412.7	0.75618
S1	1000000	1.6265
S2	47413000	1.4624

Table 5 illustrates the fatigue life and safety factor of the baseline and optimized blades S1 and S2. However, with a safety factor of 1.4624 and a fatigue life of 47,413,000 cycles, design S2 exhibits an even more astounding improvement. According to the findings, both optimized designs had much greater fatigue life and safety factors than the baseline blade, demonstrating enhanced robustness and dependability in the face of cyclic stress. Because they demonstrate developments in design optimization targeted at improving the performance and lifetime of wind turbine blades, these studies are significant to the wind turbine industry.

6.3. Experimental Results

The setup was installed in such a way that the real-time data was acquired from sensors at an interval of 0.001 sec. The displacement and acceleration data for the baseline and optimized blade are shown in Fig 13. This data was then used to draw the spectrum vs frequency chart using a fast Fourier transform (FFT). The data produced using FFT is compared in Fig 14. The obtained results show a marked increase in 1st modal frequency of the optimized blade.

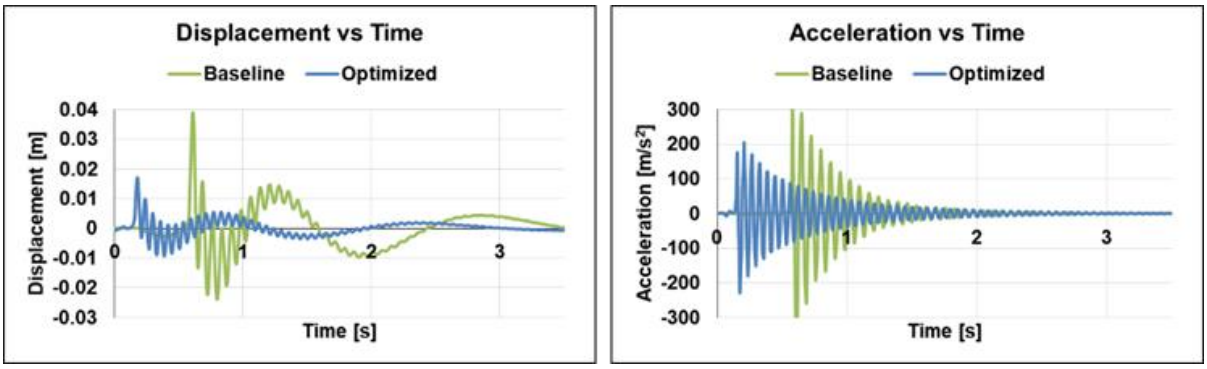

Fig 13. Displacement and acceleration data acquired from experimental testing.

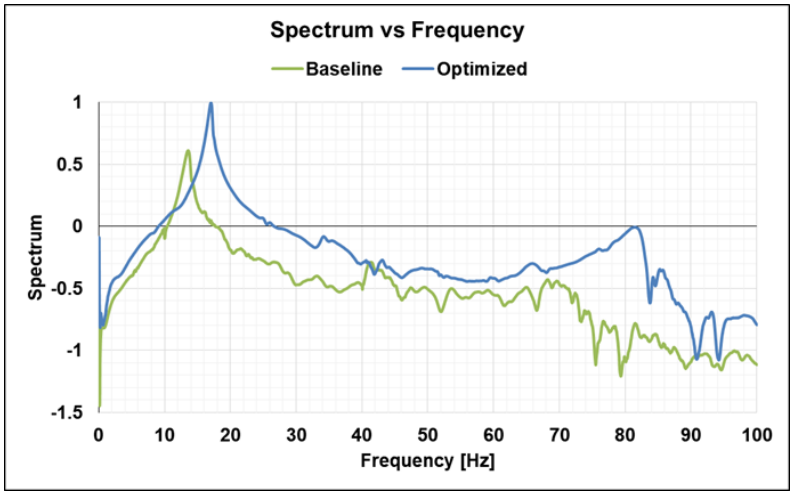

Fig 14. FFT data comparison for baseline and optimized blade.

6.4. Validation of Numerical and Experimental Results

The modal frequencies of the optimized blade computed from FEM analysis are also shown in Fig 15. The values of FEM and experimental show good agreement with less than 10% error. It can be seen that the mass of the accelerometer has a significant impact on the final findings of the experiment. Therefore, it is thought that the discrepancy between the results obtained using Finite Element Method (FEM) and the actual experimentation is attributed to the mass of the accelerometer. However, this aspect is not currently being examined in study due to the constraints of restricted scope and available resources. The discrepancy can be reduced by up to 10% with adjustments made to the experimental equipment in future research. The additions of the hardware mass can affect the result of modal analysis significantly. However, it is worth mentioning that the selection between the accelerometer was based on well-balanced trade-off between sensitivity of the sensor and mass. Considering the available resources the sensor provided the necessary sensitivity for accurate measurement. Further, it is to be mentioned that the mass of the accelerometer is almost 10% of the total mass of the accelerometer, which is slightly larger than the acceptable limit. The discrepancy in the results have been noted and efforts will be made to be considered in future.

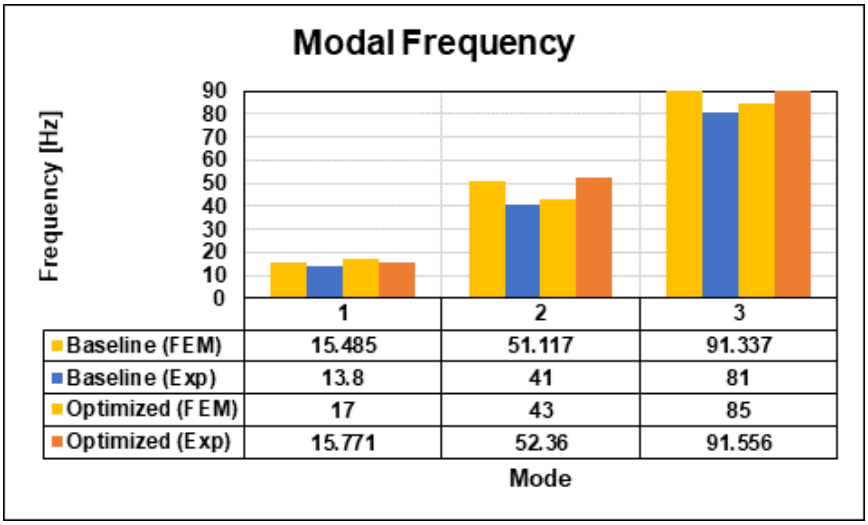

Fig 14. Modal Frequencies comparison of experimental and numerical analysis data.

7. Conclusions

This research illustrates that numerical models and actual experiments can examine a 3D-printed scaled wind turbine blade's modal and fatigue life. Our extensive research of a 1:3.75-scale carbon fiber-reinforced polylactic acid (PLA) model showed structural integrity and dynamic features. Geometric and dynamic scaling principles allow our models to accurately predict full-scale blade behavior. Mode shapes and frequencies are shown via ANSYS Workbench modal analysis, while fatigue life analysis shows durability under realistic load. Experimental testing confirms our numerical predictions that design adjustments increase structural integrity. This shows how additive manufacturing and design optimization can improve wind energy infrastructure.

The revised blade's 1st modal frequency improves dramatically, indicating structural integrity improvements, according to the experiments. The first three modes of the modified blade have frequencies greater than baseline, indicating our design improvements work. The computed modal frequencies are also validated by experimental modal frequencies with FEA analysis, which matches numerical simulations within 10%. In order to confirm the predictive capabilities of computer models with respect to behavior in the real world, rigorous validation methods need to be applied. The results from this study will further help in the better understanding of blade behavior in service and thus provide avenues in improving wind energy infrastructure efficiency, durability and sustainability. These become part of the analysis either for future recommendations or takeaways. New materials and manufacturing processes might enhance the efficiency and lifespan of wind turbine blades.

References

[1] H. Jokar, M. Mahzoon, R. Vatankhah, Dynamic modeling and free vibration analysis of horizontal axis wind turbine blades in the flap-wise direction, *Renewable energy*, Vol. 146, pp. 1818-1832, 2020.

[2] C. Kong, H. Kim, J. Kim, A study on structural and aerodynamic design of composite blade for large scale HAWT system, *Final report, Hankuk Fiber Ltd*, 2000.
[3] D. Le Gourieres, 2014, *Wind power plants: theory and design*, Elsevier,
[4] R. M. Mayer, Design of composite structures against fatigue: applications to wind turbine blades, *(No Title)*, 1996.
[5] S. A. Khan, H. A. Khan, A. Khan, S. Salamat, S. S. Javaid, R. M. A. Khan, Investigation of the mechanical behavior of FDM processed CFRP/Al hybrid joint at elevated temperatures, *Thin-Walled Structures*, Vol. 192, pp. 111135, 2023.
[6] F. Emami, M. Z. Kabir, Performance of composite metal deck slabs under impact loading, in *Proceeding of*, Elsevier, pp. 476-489.
[7] A. A. F. Ogaili, A. A. Jaber, M. N. Hamzah, Wind turbine blades fault diagnosis based on vibration dataset analysis, *Data in Brief*, Vol. 49, pp. 109414, 2023.
[8] A. Olabi, K. Obaideen, M. A. Abdelkareem, M. N. AlMallahi, N. Shehata, A. H. Alami, A. Mdallal, A. A. M. Hassan, E. T. Sayed, Wind energy contribution to the sustainable development goals: case study on London array, *Sustainability*, Vol. 15, No. 5, pp. 4641, 2023.
[9] S. A. Khan, H. Liaqat, F. Akram, H. A. Khan, Development of a design space for dissimilar materials joining in aerospace applications, *The Aeronautical Journal*, Vol. 128, No. 1324, pp. 1284-1301, 2024.
[10] M. Nazim, H. A. Khan, S. A. Khan, H. Liaqat, K. Rehman, Design, Development, and Performance Evaluation of FDM-Based Fastening Techniques for Single-Lap Joints, *JOM*, Vol. 76, No. 2, pp. 930-940, 2024.
[11] F. Emami, A. J. Gross, Mechanical Properties of Hierarchical Beams for Large-Scale Space Structures, in *Proceeding of*, 0384.
[12] T. Faber, M. Klose, Experiences with certification of offshore wind farms, in *Proceeding of*, ISOPE, pp. ISOPE-I-06-352.
[13] C. Stork, C. Butterfield, W. Holley, P. H. Madsen, P. H. Jensen, Wind conditions for wind turbine design proposals for revision of the IEC 1400-1 standard, *Journal of Wind Engineering and Industrial Aerodynamics*, Vol. 74, pp. 443-454, 1998.
[14] D.-P. Molenaar, S. Dijkstra, Modeling the structural dynamics of flexible wind turbines, in *Proceeding of*, Routledge, pp. 234-237.
[15] M. Lillico, R. Butler, Finite element and dynamic stiffness methods compared for modal analysis of composite wings, *AIAA journal*, Vol. 36, No. 11, pp. 2148-2151, 1998.
[16] S. Poole, R. Phillips, Rapid prototyping of small wind turbine blades using additive manufacturing, in *Proceeding of*, IEEE, pp. 189-194.
[17] M. S. Davis, M. R. Madani, 3D-printing of a functional small-scale wind turbine, in *Proceeding of*, IEEE, pp. 1-6.
[18] M. Rouway, M. Tarfaoui, N. Chakhchaoui, L. E. H. Omari, F. Fraija, O. Cherkaoui, Additive manufacturing and composite materials for marine energy: case of tidal turbine, *3D Printing and Additive Manufacturing*, Vol. 10, No. 6, pp. 1309-1319, 2023.
[19] H. A. Porto, C. A. Fortulan, A. J. V. Porto, R. H. Tsunaki, Geometric Analysis of Small Wind Turbine Blades Manufactured by Additive Manufacturing, *Journal of Aerospace Technology and Management*, Vol. 14, pp. e1022, 2022.
[20] U. Singh, M. Lohumi, H. Kumar, Additive manufacturing in wind energy systems: A review, in *Proceeding of*, Springer, pp. 757-766.
[21] P. Murdy, J. Dolson, D. Miller, S. Hughes, R. Beach, Leveraging the advantages of additive manufacturing to produce advanced hybrid composite structures for marine energy systems, *Applied Sciences*, Vol. 11, No. 3, pp. 1336, 2021.
[22] S. Sivamani, M. Nadarajan, R. Kameshwaran, C. D. Bhatt, M. T. Premkumar, V. Hariram, Analysis of cross axis wind turbine blades designed and manufactured by FDM based additive manufacturing, *Materials Today: Proceedings*, Vol. 33, pp. 3504-3509, 2020.
[23] A.-P. Chiriță, P.-P. Bere, R. I. RĂDOI, L. Dumitrescu, Aspects regarding the use of 3D printing technology and composite materials for testing and manufacturing vertical axis wind turbines, *Mater. Plast*, Vol. 56, No. 4, 2019.
[24] K. Bassett, R. Carriveau, D.-K. Ting, 3D printed wind turbines part 1: Design considerations and rapid manufacture potential, *Sustainable Energy Technologies and Assessments*, Vol. 11, pp. 186-193, 2015.
[25] C. Zhu, T. Li, M. M. Mohideen, P. Hu, R. Gupta, S. Ramakrishna, Y. Liu, Realization of circular economy of 3D printed plastics: A review, *Polymers*, Vol. 13, No. 5, pp. 744, 2021.

[26] M. Dinar, D. W. Rosen, A design for additive manufacturing ontology, *Journal of Computing and Information Science in Engineering*, Vol. 17, No. 2, pp. 021013, 2017.
[27] H. Schappo, L. Piaia, D. Hotza, G. V. Salmoria, Selective Laser Sintering of Biomaterials and Composites State of the Art and Perspectives, in *Proceeding of*, Trans Tech Publ, pp. 278-283.
[28] T. D. Ngo, A. Kashani, G. Imbalzano, K. T. Nguyen, D. Hui, Additive manufacturing (3D printing): A review of materials, methods, applications and challenges, *Composites Part B: Engineering*, Vol. 143, pp. 172-196, 2018.
[29] P. Dudek, FDM 3D printing technology in manufacturing composite elements, *Archives of metallurgy and materials*, Vol. 58, No. 4, pp. 1415--1418, 2013.
[30] Y. Zhai, D. A. Lados, J. L. LaGoy, Additive manufacturing: making imagination the major limitation, *Jom*, Vol. 66, pp. 808-816, 2014.
[31] S. C. Daminabo, S. Goel, S. A. Grammatikos, H. Y. Nezhad, V. K. Thakur, Fused deposition modeling-based additive manufacturing (3D printing): techniques for polymer material systems, *Materials today chemistry*, Vol. 16, pp. 100248, 2020.
[32] J.-Y. Lee, J. An, C. K. Chua, Fundamentals and applications of 3D printing for novel materials, *Applied materials today*, Vol. 7, pp. 120-133, 2017.
[33] A. K. Zarzoor, A. A. Shandookh, A. A. Jaber, Analysis of 5 MW NREL Wind Turbine Using Qblade Software, in *Proceeding of*, IEEE, pp. 1-7.
[34] H. Canet, P. Bortolotti, C. L. Bottasso, On the scaling of wind turbine rotors, *Wind Energ. Sci. Discuss., https://doi. org/10.5194/wes-2020-66, in review*, 2020.
[35] H. Petersen, The scaling laws applied to wind turbine design, *Wind Engineering*, pp. 99-108, 1984.
[36] N. Sergiienko, L. Da Silva, E. Bachynski-Polić, B. Cazzolato, M. Arjomandi, B. Ding, Review of scaling laws applied to floating offshore wind turbines, *Renewable and Sustainable Energy Reviews*, Vol. 162, pp. 112477, 2022.
[37] F. Emami, M. Z. Kabir, Strength prediction of composite metal deck slabs under free drop weight impact loading using numerical approach and data set machine learning, *Scientia Iranica*, 2023.
[38] N. H. Baharin, R. A. Rahman, Effect of accelerometer mass on thin plate vibration, *Jurnal Mekanikal*, 2009.